Biochemistry and Biophysics Reports 6 (2016) 32–38

Contents lists available at ScienceDirect

Biochemistry and Biophysics Reports

journal homepage: www.elsevier.com/locate/bbrep

Impedance-based analysis of mu opioid receptor signaling and underlying mechanisms

David Thirkettle-Watts

Defence Science and Technology Group, 506 Lorimer St, Fishermans Bend, Victoria, Australia

ARTICLE INFO

Article history:
Received 15 January 2016
Received in revised form
29 February 2016
Accepted 1 March 2016
Available online 3 March 2016

Keywords:
Impedance
Opioid
GPCR
Real-time cellular analysis
G-protein
Label-free

ABSTRACT

The mu opioid receptor is a G-protein coupled receptor able to signal through the $G\alpha_{i/o}$ class of G-protein and β-arrestin pathways, stimulating down-stream effector pathways. Signaling bias occurs when different receptor agonists lead to different signaling outcomes. Traditionally these have been studied using end-point assays. Real-time cellular analysis platforms allow for the analysis of the holistic effects of receptor activation as an integrated output. While this allows for different ligands to be compared rapidly, the cellular mechanisms underlying the signal are not well described. Using an impedance based system, the impedance responses for two opioid ligands, morphine and DAMGO were examined.

The impedance responses for these two agonists, while showing similar features, were distinct from each other. Some of the mechanisms underlying the mu opioid receptor coupled impedance changes were investigated. It was found that the response is a result of discrete cellular processes, including G-protein signaling and protein kinase phosphorylation.

1. Introduction

The mu opioid receptor (MOR) is a member of the opioid family of receptors and the large G-protein coupled receptor (GPCR) superfamily. Activation of this receptor results in a GDP/GTP exchange at specific G-proteins with the resulting release of the G-protein subunits leading to stimulation of downstream effector pathways. Receptor activation can also result in the recruitment of β-arrestin leading to receptor internalisation and the activation of a G-protein independent signaling pathway. Agonists can activate different pathway subsets leading to signaling bias [1,2].

The opioid agonists [D-Ala^2, NMe-Phe^4, Gly-ol^5]-enkephalin (DAMGO) and morphine are both MOR agonists which have been shown to exhibit bias in their signaling [3,4]. One measure of this bias is the induction of receptor internalisation. In the majority of cell types, treatment with DAMGO leads to internalisation while morphine shows relatively less internalisation [5–8]. A second illustration of bias is the observation that in β-arrestin2 knockout mice, morphine analgesia is enhanced while respiratory depression is reduced [9].

In addition to ligand bias changing the level at which pathways can be activated, the outcomes of receptor stimulation can be influenced by type or state of a cell. There is also the possibility of unexpected pathways being activated causing the full set of effects to be missed [3,5,6,10,11]. A system with a read-out capturing the whole cell response to receptor activation will allow a holistic comparison of agonists. Label-free real-time cellular analysis (RTCA) platforms allow an approach naïve to the actual mechanisms activated but instead capture an integrated whole-cell output. This can include cell processes that have not previously been described [11,12].

One RTCA platform uses an impedance based assay, which measures the change in impedance over time produced by cultured cells grown on an array of interdigitated circuits on the base of a 96-well microplate. This provides an output integrating the whole cell signals that lead to a change in impedance resulting from ligand stimulation. The assay is label-free and provides for a real-time analysis of cell events [13,14]. This technique is starting to be utilised to examine GPCR ligands with a goal of allowing an unbiased method of classifying ligands into discrete pharmacological categories and to give an indication of their signaling bias [12,15]. Most of the underlying mechanisms that lead to ligand-induced cellular morphological changes and a change in cellular impedance are not well understood. A better understanding of what cellular processes underlie impedance profiles will allow a more confident assessment of compounds and the prediction of their properties. This may have applications such as the screening of compounds for desirable properties.

Here the impedance profiles generated by the opioid agonists DAMGO and morphine were compared using Chinese Hamster Ovary (CHO) cells stably overexpressing the MOR and some of the cellular processes behind the impedance response were investigated. In particular the contribution of kinase signaling cascades to the response

Abbreviations: MOR, mu opioid receptor; GPCR, G-protein coupled receptor; CI, cell index; RTCA, real-time cellular analysis; CHO, Chinese hamster ovary; FCS, foetal calf serum; DAMGO, [D-Ala^2, NMe-Phe^4, Gly-ol^5]-enkephalin

E-mail address: David.Thirkettle-Watts@dsto.defence.gov.au

http://dx.doi.org/10.1016/j.bbrep.2016.03.002

was examined. The results showed that individual opioid agonists can lead to distinct impedance profiles. The impedance response is the result of discrete cellular processes which act in a time-dependent manner. Part of this response is due to the contributions of the AKT1/2/3 pathway, in the early stages of the response and the ERK1/2 pathway at later stages of the response.

2. Material and methods

2.1. Cell culture

CHO cells stably expressing the human MOR were a gift from Dr. Meritxell Canals [16]. Cell culture medium and foetal calf serum were purchased from Gibco. Cells were maintained in DMEM medium supplemented with 4.5 g/l D-Glucose and 10% foetal calf serum (FCS) and incubated in a humidified incubator at 37 °C with 5% CO_2.

2.2. Impedance measurement

The xCELLigence system (ACEA Biosciences, San Diego) was used to measure changes in cellular impedance resulting from stimulation with a ligand in 96-well E-Plates [13]. The E-Plate has electrode arrays integrated into the bottom of the wells which allow for the measurement of the impedance conferred by cells growing on this surface. Changes in the measured impedance are defined by a unit-less cell index (CI). Prior to the addition of cells to the E-Plate, a CI measurement was taken in the presence of 100 µl growth medium to determine the background CI value for each well. This was subtracted from the subsequent CI values as they were collected following cell attachment. Cells were seeded at a density of 2×10^4 cells/well and cultured overnight in growth medium. After approximately 24 h, the cell medium was replaced with serum free DMEM and the volume of medium in the wells was adjusted to 180 µl for assays only requiring ligand or 160 µl for assays requiring an additional treatment and incubated overnight for approximately 16 h.

The E-plate was kept in the incubator for the duration of the experiments. For the addition of compounds, E-Plate lid was replaced with the RTCA Protector Shield 96 (allowing access to the wells whilst the E-Plate is actively monitored in the cradle) and the E-Plate was equilibrated for 30 min. Compounds were diluted in serum-free medium to a 10× concentration, and added using an automated multichannel pipette (20 µl /well). For agonist addition, the sampling frequency was increased to the maximum possible with CI values collected at 10 s intervals for a minimum period of 1 h.

For analysis, CI values were normalised by dividing by the cell index at the time immediately prior to ligand addition (time = 0 min). Baseline corrections were carried out by subtracting the cell index obtained from vehicle-treated cells. Between four and eight replicates were used for each treatment per experiment.

2.3. Kinase activation assay

Cells were plated and grown in 96-well plates at a density of 4×10^4 cells/well. The cells were cultured and treated with ligands as described for the impedance measurement assay. ERK1/2 and AKT1/2/3 phosphorylation were measured using the ERK1/2 (Thr202/Tyr204), AKT1/2/3 Thr308 and AKT1/2/3 Ser473 AlphaScreen Surefire kit (Perkin Elmer). Cells were treated with 10 µM of either DAMGO or morphine for varying periods of time required for the experiment, then immediately lysed in 100 µl of the supplied lysis buffer with shaking for 10 min at room temperature. Plates were then sealed and stored at −20 °C. After thawing on ice, 5 µl were transferred to a 384-well ProxiPlate (Perkin Elmer) to be used for the phosphorylation assay as per the manufacturer's instructions.

2.4. Data analysis

Graphing and analysis of results were performed using RTCA software (v1.2.1.1002) provided by Roche Applied Science with the xCELLigence System and Prism5 (GraphPad, CA, USA).

2.5. Materials

U0126, GSK2334470 and FB-124 were purchased from Tocris, DAMGO [D-Ala^2, NMe-Phe^4, Gly-ol^5]-enkephalin) and Morphine sulphate were purchased from Sigma.

3. Results and discussion

3.1. Impedance profiles

Real-time measurement of impedance results in a profile which represents the integration of multiple signal events stimulated by receptor activation. The MOR is known to activate two signaling pathways: $G\alpha_{i/o}/G\beta\gamma$ and β-arrestin. To determine the profiles resulting from opioid receptor stimulation and to investigate whether impedance measurements can distinguish between different agonists, CHO cells stably overexpressing the human MOR were treated with either DAMGO or Morphine.

The stimulation of cells using each agonist leads to a concentration-dependent, multi-featured, impedance response (Fig. 1). The treatment of cells with either DAMGO or morphine resulted in profiles that displayed broadly similar features, although each agonist displayed unique characteristics (Fig. 1A). The impedance profiles could be divided into several phases. Stimulation using both agonists resulted in a rapid rise in CI (rapid ascending phase), a peak (major peak) and then an initial decay (first decay). This was followed by a "second ascending phase" and a second peak (minor peak). Finally a "second decay" lead to a "plateau phase" in which the CI is maintained at a level higher than the initial baseline.

The rapid ascending phase and major peak for each agonist showed a high degree of similarity. In contrast, the region of the profile representing the minor peak showed differences. In particular, the CI of this region was higher for cells stimulated by morphine compared to DAMGO.

To demonstrate that this response was due to MOR activation, cells were treated with the pan-antagonist naloxone (10 µM) prior to agonist addition. Treatment with naloxone resulted in the complete inhibition of the impedance response of both DAMGO and morphine (Fig. 1B and C). Furthermore, the dose-response curve elicited by both agonists was moved to the right with increasing concentrations of Naloxone, indicating a competitive antagonism (data not shown).

Previous studies have examined the impedance response elicited by the activation of several GPCR's and have shown a diverse range of impedance profiles. These include activation of the β_2-Adrenergic receptor, the niacin receptor GPR109A and the chemokine receptor CXCR3 [12,15,17]. These reports showed that the stimulation of each of these receptors resulted in a specific changes in cellular impedance and that the response for an individual receptor was dependent on the agonist used. The impedance profiles generated by the stimulation of the MOR were distinct from those previously published, although there were similarities with the two other $G_{i/o}$ coupled receptors, GPR109A and CXCR3. All three of these receptors have profiles which contain a feature similar to the major peak shown here.

The impedance profiles were concentration-dependent with different features of the impedance profile showing differential responses (Fig. 1D and E). This indicates that separate signaling events were involved in the development of the impedance responses over time. This was demonstrated by generating dose-response curves for two of the features of the profile; the major and minor peaks

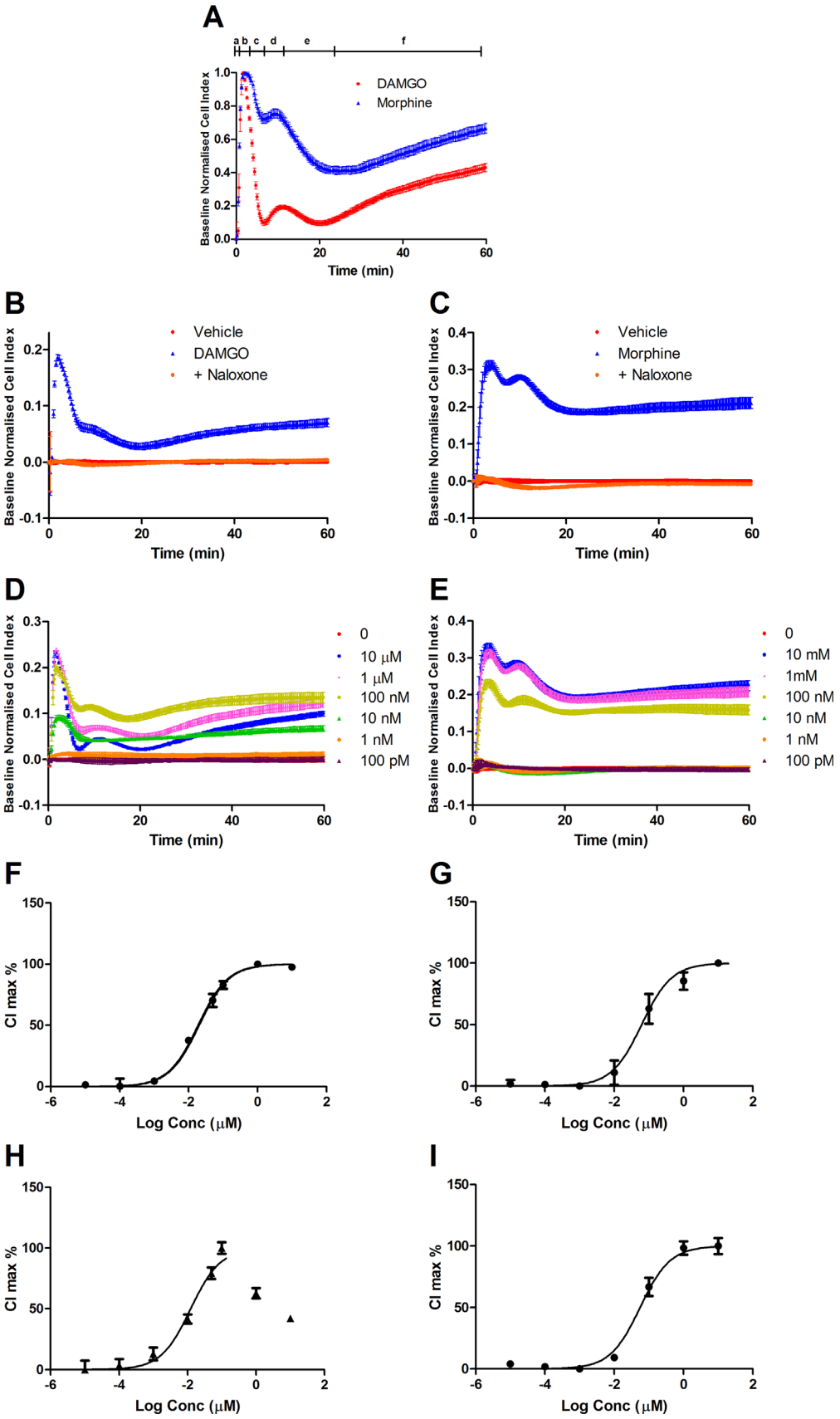

Fig. 1. Ligand induced changes in cellular impedance mediated through the MOR. (A) Changes in cellular impedance in CHO-MOR cells were measured over time following treatment with DAMGO or morphine. The phases of the response are indicted; rapid ascending phase (a), major peak (b), first decay (c), minor peak (d), second decay (e) and plateau phase (f). Cells were treated with 10 μM naloxone 30 min prior to the addition of (B) 10 μM DAMGO or (C) 10 μM morphine. Cells were treated with (D) DAMGO or (*E*) morphine at the concentrations indicated, concentration-response curves of the maximum Cell Index (CI) from the first peak for (F) DAMGO and (G) morphine or the second peak for (H) DAMGO and (I) morphine were generated. For (H), data points at Log Conc. 0 and 1 μM were not included in the curve fitting. Cells were seeded at a density of 2×10^4 cells/well and maintained at 37 °C, 5% CO_2 for the duration of the experiment. Data presented is the mean of between five and eight independent experiments ± Standard deviation.

(Fig. 1F–I). In morphine-stimulated cells, both dose-response curves showed a normal sigmoidal response with EC_{50}s of 77.7 nM for the major peak and 82.4 nM for the minor peak (Fig. 1G and I). In contrast DAMGO treated cells produced an impedance profile for which the shape of the dose response curves varied at these different points (Fig. 1F and H). The major peak behaved in a normal sigmoidal fashion with an EC_{50} of 18.3 nM; the minor peak showed a biphasic response. At DAMGO concentrations below 100 nM, a normal sigmoidal response curve was seen (EC_{50} of 12.7 nM). At higher concentrations, increases in the DAMGO concentration lead to a decrease in CI. This indicates that there may be competing signals underlying the change in impedance, the impedance profile being the combined effect of all of the pathways and processes that contribute to the change in the cellular impedance.

To test whether the observed impedance response included underlying mechanisms coupled to the G-protein pathway, the function of the G-proteins was specifically inhibited using pertussis toxin (PTX), which uncouples the receptor from $G\alpha_{i/o}$ proteins [18] and gallein, which inhibits the interactions of $G\beta\gamma$ with its substrates [19,20]. Stimulation of PTX-pretreated cells with DAMGO and morphine resulted in a loss of the impedance response (Fig. 2A and B). In contrast, the gallein pre-treatment lead to major peaks reduced to 45% (SEM ± 4.2) and 38% (SEM ± 8.2) that of non-treated cells, for DAMGO and morphine respectively (Fig. 2C and D). The minor peak for both of the treatments was reduced but still visible, while the plateau phase was completely lost. These data suggest that the entire MOR impedance signal is reliant on the presence of a functional $G\alpha_{i/o}$. This includes the β-arrestin mediated response. The recruitment of β-arrestin is stimulated by the phosphorylation of the receptor via G-protein receptor kinases (GRK), recruited to the receptor by the free $G\beta\gamma$ [21].

3.2. Kinase phosphorylation

The activation of MOR is known to lead to the activation of MAPK pathways. While ERK1/2 is the most widely described, other pathways have also been implicated in the opioid response [22–24]. The activation of several MAPK, the NF-κB and AKT signaling pathways in response to the opioid treatments were measured using Alphascreen antibody-based assays. There was no evidence of the activation of p38, JNK or NF-κB (data not shown), whereas ERK1/2 and AKT1/2/3 displayed phosphorylation in response to MOR activation in a time dependent manner (Fig. 3).

Following both DAMGO and morphine treatments, the phosphorylation of ERK1/2 was detected using an antibody binding to the Threonine 202/Tyrosine 204 phosphorylated epitope. Phosphorylation of ERK1/2 was detected after two minutes and peaked at five minutes (Fig. 3A and D). The activation of the AKT1/2/3 pathway was investigated using two assays to detect either the phosphorylated Threonine 308 (Thr308) or Serine 473 (Ser473) sites of AKT1, 2 and 3. The phosphorylation at both of these sites occurred rapidly in cells treated with DAMGO or morphine. For cells treated with DAMGO, AKT phosphorylation peaked at two minutes and rapidly decreased (Fig. 3B and C). For cells treated with morphine, the peak in AKT phosphorylation at both sites occurred at five minutes and was sustained for longer (Fig. 3E and F).

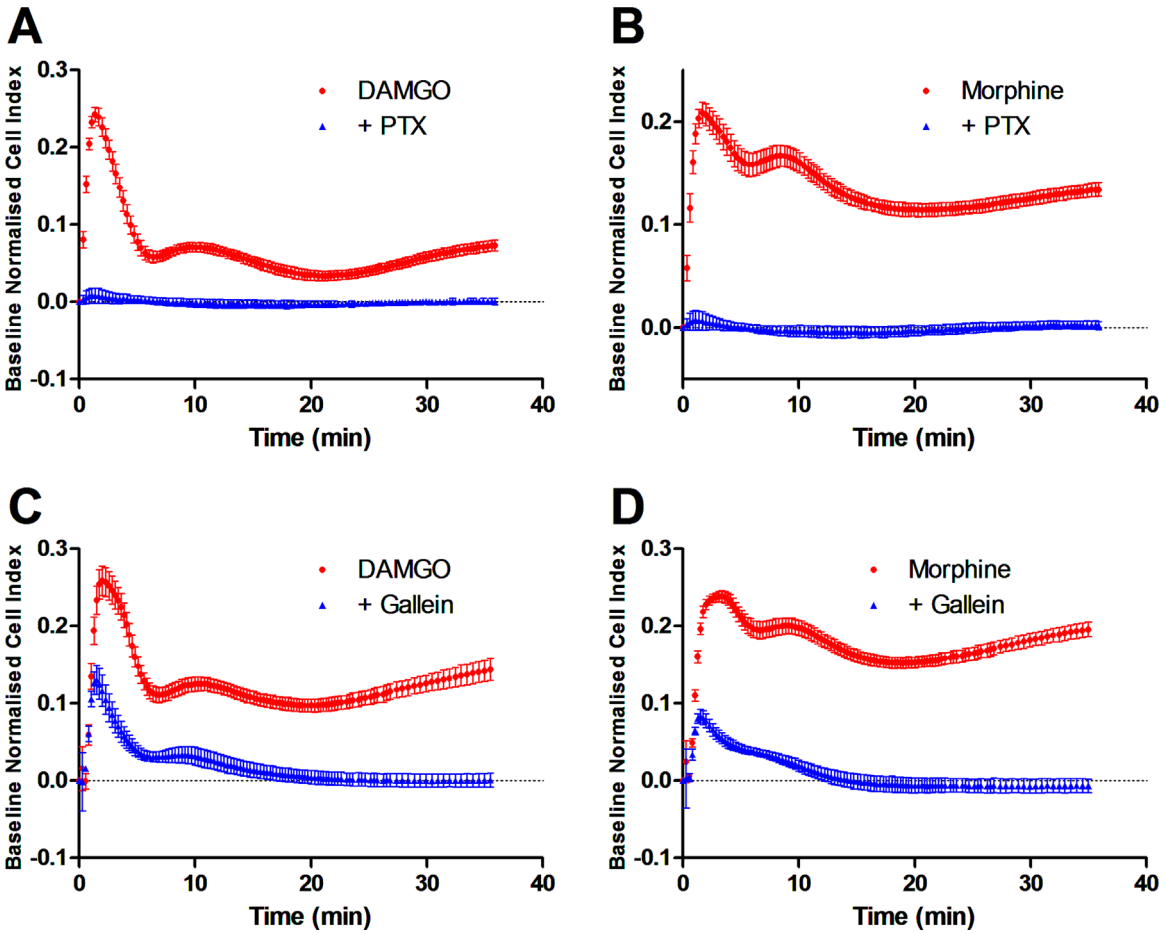

Fig. 2. Changes in opioid induced changes in cellular impedance are mediated by $G\alpha_{i/o}$ and $G\beta\gamma$. CHO-MOR cells were grown overnight in the presence or absence of 100 ng/ml PTX and then treated with 10 μM (A) DAMGO or (B) morphine. Cells were treated with 100 μM gallein for 1 h and then Treated with 10 μM (C) DAMGO or (D) morphine. Cells were seeded at a density of 2×10^4 cells/well and maintained at 37 °C, 5% CO_2 for the duration of the experiment. Data presented is the mean of between four and six independent experiments ± Standard deviation.

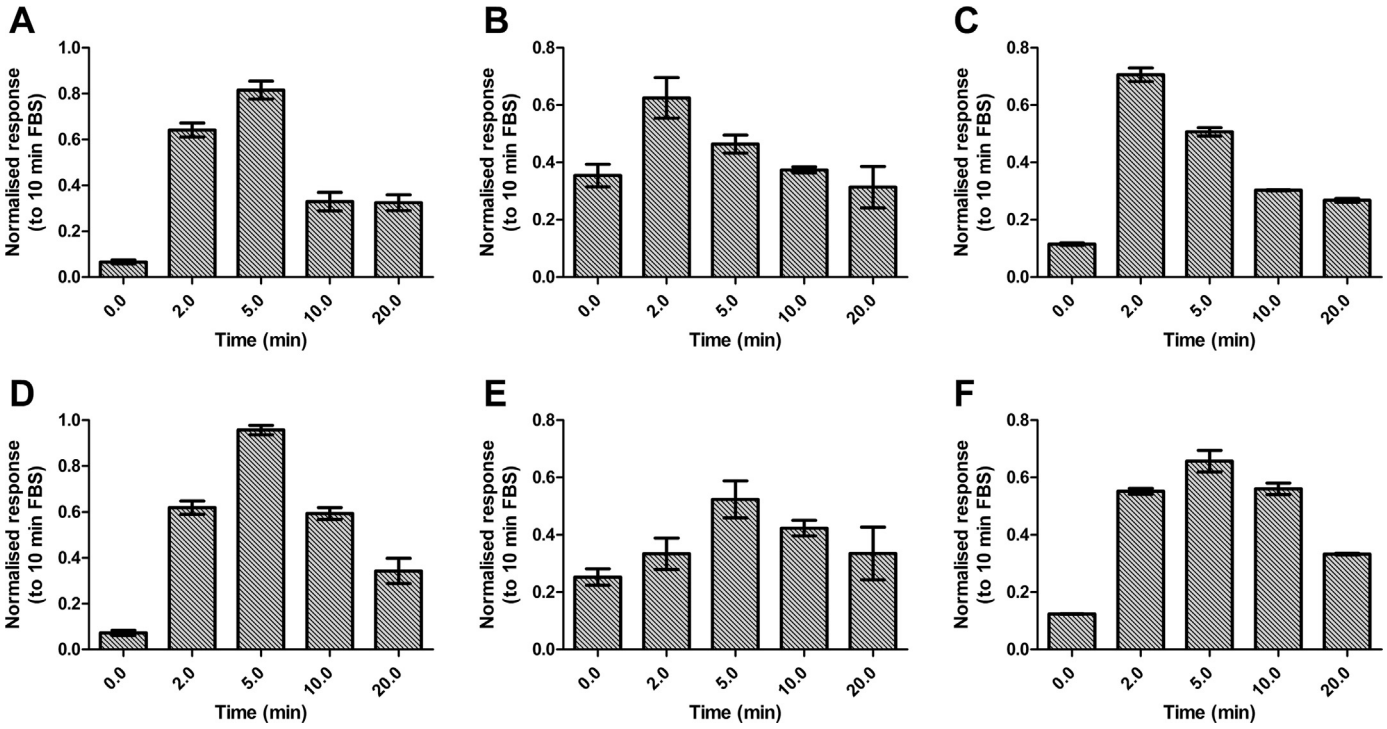

Fig. 3. Time dependent ligand induced protein phosphorylation in CHO-MOR cells. Cells were treated with 10 μM DAMGO and assayed for ERK1/2 phosphorylation (A), AKT1/2/3 phosphorylation at Thr308 (B) or AKT1/2/3 phosphorylation at Ser473 (C). Cells were treated with 10 μM morphine and assayed for ERK1/2 phosphorylation (D), AKT1/2/3 phosphorylation at Thr308 (*E*) or AKT1/2/3 phosphorylation at Ser473 (F). Data is normalised to the response induced by 10% FCS at 10 min and expressed as the mean ± Standard deviation of three independent experiments.

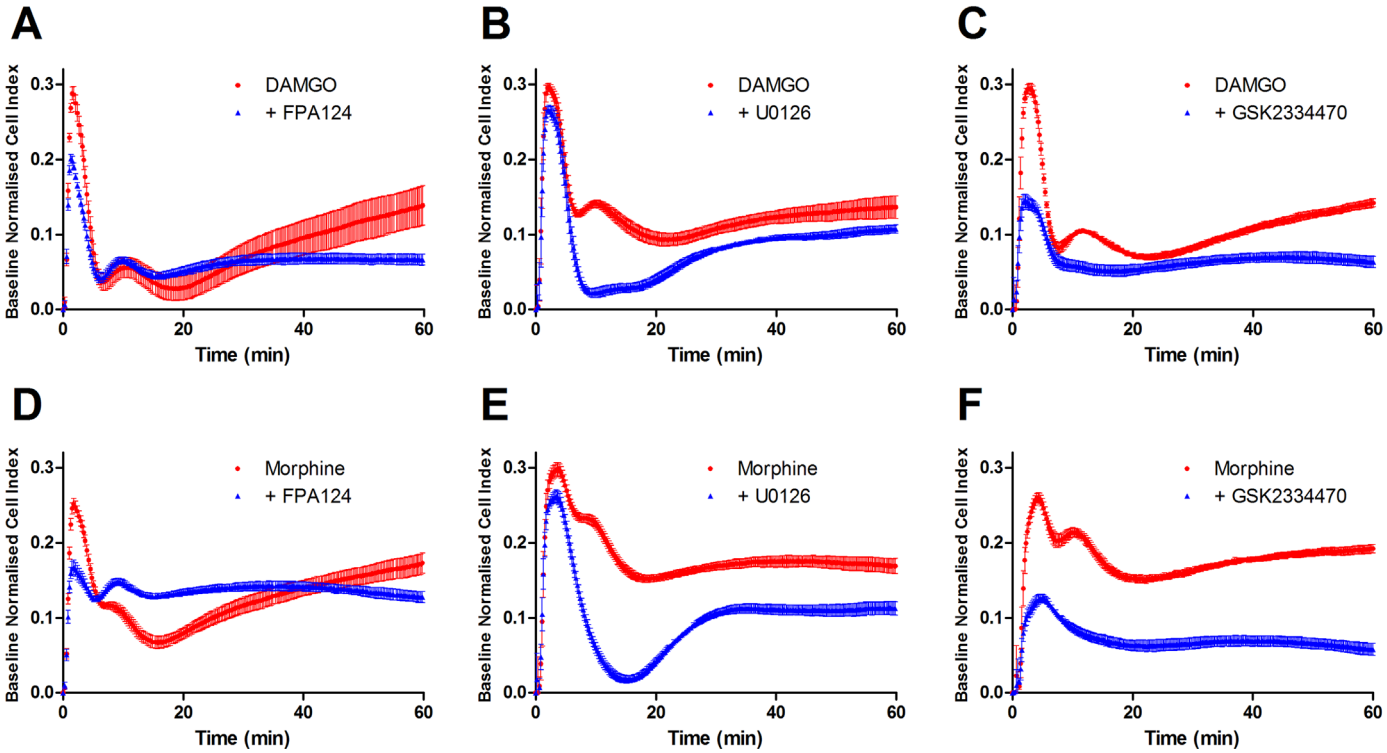

Fig. 4. The inhibition of kinase pathway components results in discreet effects on the cellular impedance. CHO-MOR cells were treated with inhibitors for 30 min before the addition of 10 μM ligand. Cells treated with 10 μM FPA124, 5 μM U0126 or 10 μM GSK2334470 were treated with DAMGO (A–C) or morphine (D–F). Cells were seeded at a density of 2×10^4 cells/well and maintained at 37 °C, 5% CO_2 for the duration of the experiment. Data presented is the mean of between four and six independent experiments ± Standard deviation.

3.3. Relationship of phosphorylation pathways to impedance profile

The contribution of these protein phosphorylation pathways to the impedance profiles was examined using three chemical inhibitors to disrupt the signaling; U0126 to block ERK1/2 phosphorylation, FPA124 to directly inhibit AKT1/2/3 and GSK2334470, an inhibitor of 3-phosphoinositide-dependent protein kinase 1 (PDK1) [25–27]. PDK1 represents a signal pathway branch point, with the ability to phosphorylate MEK (the kinase responsible for ERK phosphorylation) on Ser222 and Ser226 [28,29] and AKT on Thr308 [30,31].

When FPA124-treated cells were stimulated with either DAMGO or morphine, the effect on the impedance response was predominantly on the amplitude of the major peak and the plateau phase (Fig. 4A and D). The major peak was reduced to 64% and 70% of the maximum CI for DAMGO and morphine respectively while the plateau phase was lost. There was no effect on the slope ascending phase or the secondary peak. In contrast, the pre-treatment of cells with U0126 resulted in an agonist-stimulated impedance profile showing only a minor effect on the amplitude of the major peak (more than 90% of maximum CI), little effect on the plateau phase but an complete loss of the second peak (Fig. 4B and E). Inhibition of PDK1 with GSK2334470 resulted in an impedance response that resembled a combination of the two previous profiles (Fig. 4C and F). The amplitude of the major peak compared to the uninhibited cells was reduced to 57% for DAMGO and 56% for morphine and the secondary peak and plateau phase for both was completely lost.

These data suggest that the ERK1/2 and AKT1/2/3 pathways largely contributed to separate features of the impedance response. This contribution aligns with the temporal activation of the two proteins. The initial major peak occurs between 2 and 3 min and is most affected by inhibition of the AKT pathway. The ERK pathway provides only a minor contribution to the major peak, but is significant in the formation of the minor peak which occurs at approximately 10 min. These results are consistent with the timing of AKT and ERK phosphorylation. There is some evidence (data not shown) that there may be subtle differences in the timing of these impedance profile features between the two agonists which bears further investigation.

In the impedance profiles presented, the second minor peak is mainly the result of the activation of the ERK pathway. This region also provides the major difference between the impedance profiles generated by the two agonists. This implies that, although both agonists lead to ERK1/2 phosphorylation, there are differences in the mechanism by which this is achieved. GPCR coupled ERK1/2 phosphorylation can be stimulated via two mechanisms, G-protein or β-arrestin coupled [26]. A major contributor to receptor bias described for GPCRs has been shown to be differences in the activation of these two pathways [32,33]. Furthermore, the activation of ERK1/2 is further complicated by the ability of ERK1/2 to function either in the cytosol or translocate to the nucleus [26,34]. It is likely that the different ERK related impedance signatures have a basis in the different levels of coupling to one of the ERK pathways [3]. The impedance profiles show both a difference in both the shape of the curve and the dose-response at this region. Morphine stimulation results in a peak with a higher CI and a sigmoidal dose-response curve while DAMGO stimulation leads to a peak with a lower peak CI and dose-response curve with two phases. This minor peak has also been observed to be more variable in both shape and relative amplitude than any of the other phases of the profiles (data not shown). This indicates the possibility of dynamic cellular processes, including the recruitment of interacting proteins such as regulators of G protein signaling (RGS), having an influence on the impedance response [3].

This report describes the application of an electrical impedance RTCA assay to study the MOR mediated signaling stimulated by morphine and DAMGO. While this work focused on two kinase phosphorylation pathways, it is clear that there are other mechanisms which contribute to the impedance profiles. Further effort will elucidate the additional mechanisms that lead to changes in impedance. It is likely that factors such as receptor internalisation and modulation of ion channels will be contributors. The study demonstrated that distinct impedance profiles can result from different opioid agonists acting on the same cell type. This opens up the possibility for opioid compounds to be grouped into pharmacological classes based on their impedance profiles and for this system to be used to predict signal bias and agonist properties.

Acknowledgment

The author would like to thank David Mawdsley and Peter Gray for critically reading the manuscript.

Appendix A. Transparency document

Transparency document associated with this article can be found in the online version at http://dx.doi.org/10.1016/j.bbrep.2016.03.002.

References

[1] I. Charfi, N. Audet, H. Bagheri Tudashki, G. Pineyro, Identifying ligand-specific signalling within biased responses: focus on δ opioid receptor ligands, Br. J. Pharm. 172 (2015) 435–448.
[2] T. Kenakin, Functional selectivity and biased receptor signaling, J. Pharm. Exp. Ther. 336 (2011) 296–302.
[3] E. Kelly, Efficacy and ligand bias at the μ-opioid receptor, Br. J. Pharmacol. 169 (2013) 1430–1446.
[4] S.L. Borgland, M. Connor, P.B. Osborne, J.B. Furness, M.J. Christie, Opioid agonists have different efficacy profiles for G protein activation, rapid desensitization, and endocytosis of mu-opioid receptors, J. Biol. Chem. 278 (2003) 18776–18784.
[5] J. Zhang, S.S.G. Ferguson, L.S. Barak, S.R. Bodduluri, S.A. Laporte, P.Y. Law, M. G. Caron, Role for G protein-coupled receptor kinase in agonist-specific regulation of μ-opioid receptor responsiveness, PNAS 95 (1998) 7157–7162.
[6] S. Schulz, D. Mayer, M. Pfeiffer, R. Stumm, T. Koch, V. Höllt, Morphine induces terminal μ-opioid receptor desensitization by sustained phosphorylation of serine-375, EMBO J. 23 (2004) 3282–3289.
[7] K.M. Raehal, C.L. Schmid, C.E. Groer, L.M. Bohn, Functional selectivity at the mu-opioid receptor: implications for understanding opioid analgesia and tolerance, Pharm. Rev. 63 (2011) 1001–1019.
[8] J.T. Williams, S.L. Ingram, G. Henderson, C. Chavkin, M. von Zastrow, S. Schulz, T. Koch, C.J. Evans, M.J. Christie, Regulation of μ-opioid receptors: desensitization, phosphorylation, internalization, and tolerance, Pharm. Rev. 65 (2013) 223–254.
[9] K.M. Raehal, L.M. Bohn, Mu opioid receptor regulation and opiate responsiveness, AAPS J. 7 (2005) E587–E591.
[10] H. Haberstock-Debic, K.-A. Kim, Y.J. Yu, M. von Zastrow, Morphine promotes rapid, arrestin-dependent endocytosis of μ-opioid receptors in Striatal neurons, J. Neurosci. 25 (2005) 7847–7857.
[11] M. Morse, E. Tran, H. Sun, R. Levenson, Y. Fang, Ligand-directed functional selectivity at the mu opioid receptor revealed by label-free integrative pharmacology on-target, PLoS One 6 (2011) e25643.
[12] W. Stallaert, J.F. Dorn, E. van der Westhuizen, M. Audet, M. Bouvier, Impedance responses reveal β2-adrenergic receptor signaling Pluridimensionality and allow classification of ligands with distinct signaling profiles, PLoS One 7 (2012) e29420.
[13] M.F. Peters, C.W. Scott, Evaluating cellular impedance assays for detection of GPCR pleiotropic signaling and functional selectivity, J. Biomol. Screen 14 (2009) 246–255.
[14] P. Scandroglio, R. Brusa, G. Lozza, I. Mancini, R. Petrò, A. Reggiani, M. Beltramo, Evaluation of Cannabinoid receptor 2 and Metabotropic glutamate receptor 1 functional responses using a cell impedance-based technology, J. Biomol. Screen 15 (2010) 1238–1247.
[15] M. Kammermann, A. Denelavas, A. Imbach, U. Grether, H. Dehmlow, C. M. Apfel, C. Hertel, Impedance measurement: a new method to detect ligand-biased receptor signaling, Biochem. Biophys. Res. Commun. 412 (2011) 419–424.
[16] G.L. Thompson, J.R. Lane, T. Coudrat, P.M. Sexton, A. Christopoulos, M. Canals, Biased Agonism of endogenous opioid peptides at the μ-opioid receptor, Mol. Pharm. 88 (2015) 335–346.
[17] A.O. Watts, D.J. Scholten, L.H. Heitman, H.F. Vischer, R. Leurs, Label-free

impedance responses of endogenous and synthetic Chemokine receptor CXCR3 agonists correlate with gi-protein pathway activation, Biochem Biophys. Res. Commun. 419 (2012) 412–418.
[18] S. Mangmool, H. Kurose, Gi/o protein-dependent and -independent actions of pertussis toxin (PTX), Toxins 3 (2011) 884.
[19] D.M. Lehmann, A.M.P.B. Seneviratne, A.V. Smrcka, Small molecule disruption of G protein βγ subunit signaling inhibits neutrophil chemotaxis and inflammation, Mol. Pharm. 73 (2008) 410–418.
[20] Y. Lin, A.V. Smrcka, Understanding molecular recognition by G protein βγ subunits on the path to pharmacological targeting, Mol. Pharm. 80 (2011) 551–557.
[21] K.L. Pierce, R.T. Premont, R.J. Lefkowitz, Seven-Transmembrane receptors, Nat. Rev. Mol. Cell Biol. 3 (2002) 639–650.
[22] D. Yin, M. Woodruff, Y. Zhang, S. Whaley, J. Miao, K. Ferslew, J. Zhao, C. Stuart, Morphine promotes Jurkat cell apoptosis through pro-apoptotic FADD/P53 and anti-apoptotic PI3K/Akt/NF-[kappa]B pathways, J. Neuroimmunol. 174 (2006) 101–107.
[23] M. Tan, W.M. Walwyn, C.J. Evans, C.-W. Xie, p38 MAPK and β–arrestin2 mediate functional interactions between endogenous μ-opioid and α2A-adrenergic receptors in neurons, J. Biol. Chem. 284 (2009) 6270–6281.
[24] P. Sánchez-Blázquez, M. Rodríguez-Muñoz, J. Garzón, Mu-opioid receptors transiently activate the Akt-nNOS pathway to produce sustained Potentiation of PKC-mediated NMDAR-CaMKII signaling, PLoS One 5 (2010) e11278.
[25] V. Barve, F. Ahmed, S. Adsule, S. Banerjee, S. Kulkarni, P. Katiyar, C.E. Anson, A. K. Powell, S. Padhye, F.H. Sarkar, Synthesis, molecular characterization, and biological activity of novel synthetic derivatives of Chromen-4-one in human cancer cells, J. Med. Chem. 49 (2006) 3800–3808.
[26] H. Zheng, Y. Zeng, X. Zhang, J. Chu, H.H. Loh, P.Y. Law, Mu-opioid receptor agonists differentially regulate the expression of miR-190 and NeuroD, Mol. Pharm. 77 (2010) 102–109.
[27] A. Najafov, Eeva M. Sommer, Jeffrey M. Axten, M.P. Deyoung, Dario R. Alessi, Characterization of GSK2334470, a novel and highly specific inhibitor of PDK1, Biochem J. 433 (2011) 357–369.
[28] S. Sato, N. Fujita, T. Tsuruo, Involvement of 3-Phosphoinositide-dependent protein kinase-1 in the MEK/MAPK signal Transduction pathway, J. Biol. Chem. 279 (2004) 33759–33767.
[29] E. Aksamitiene, A. Kiyatkin, Boris N. Kholodenko, Cross-talk between Mitogenic Ras/MAPK and survival PI3K/Akt pathways: a fine balance, Biochem Soc. Trans. 40 (2012) 139–146.
[30] D.R. Alessi, M. Andjelkovic, B. Caudwell, P. Cron, N. Morrice, P. Cohen, B. A. Hemmings, Mechanism of activation of protein kinase B by insulin and IGF-1, EMBO J. 15 (1996) 6541–6551.
[31] D.R. Alessi, S.R. James, C.P. Downes, A.B. Holmes, P.R.J. Gaffney, C.B. Reese, P. Cohen, Characterization of a 3-Phosphoinositide-dependent protein kinase which phosphorylates and activates protein kinase Bα, Curr. Biol. 7 (1997) 261–269.
[32] D. Heitzler, G. Durand, N. Gallay, A. Rizk, S. Ahn, J. Kim, J.D. Violin, L. Dupuy, C. Gauthier, V. Piketty, P. Crépieux, A. Poupon, F. Clément, F. Fages, R. J. Lefkowitz, E. Reiter, Competing G protein-coupled receptor kinases balance G protein and β-Arrestin signaling, Mol. Syst. Biol. 8 (2012) 590.
[33] P.-Y. Law, Opioid receptor signal transduction mechanisms, in: G.W. Pasternak (Ed.), The Opiate Receptors, Humana Press, New York, 2011, pp. 195–238.
[34] D. Cervantes, C. Crosby, Y. Xiang, Arrestin orchestrates crosstalk between G protein-coupled receptors to modulate the Spatiotemporal activation of ERK MAPK, Circ. Res. 106 (2010) 79–88.